ACTINOFORM CLOUDS

Overlooked Examples of Cloud Self-Organization at the Mesoscale

BY MICHAEL J. GARAY, ROGER DAVIES, CLARE AVERILL, AND JAMES A. WESTPHAL

Recent satellite surveys show that these striking 200–300-km-wide radial cloud structures are more prevalent than previously supposed.

Clouds are the most familiar aspect of our atmospheric environment. Schoolchildren around the world learn the names of the different cloud types, names that were devised just over 200 yr ago by the amateur meteorologist, Luke Howard. Clouds take their names—cirrus, cumulus, and stratus—from Latin terms that describe the way clouds appear to someone standing on the ground. Cirrus clouds resemble curls of hair, cumulus clouds look like piled-up heaps, and stratus clouds are spread out like blankets. While individual clouds may take innumerable forms, Howard's system works because the shape of clouds is not completely random, but is instead governed by some organizational principle.

Because clouds also play a significant role in determining the radiation budget of the planet and serve as an important link in the hydrological cycle, they are studied using a variety of ground-based and satellite techniques. Ground-based observers often use Howard's cloud classification system, but clouds look very different when viewed from space. This is because satellites are able to see, much more easily than a single observer on the ground, the range of scales at which clouds occur within the atmosphere.

The scale of satellite observations falls within the mesoscale, defined by Orlanski (1975), to range from a few to a few thousand kilometers. Cloud organization at the mesoscale comes about because clouds act as tracers of vertical motion within the atmosphere, which is primarily due to convection. Depending on the strength of the vertical motion, convection can be deep or shallow. Deep convection extends through the depth of the troposphere and includes mesoscale convective systems and hurricanes. Shallow convection is much weaker and typically occurs within the lowest few kilometers of the atmosphere. While deep convective systems have been extensively studied due to their impact on human life and property, shallow con-

AFFILIATIONS: GARAY—Department of Atmospheric and Oceanic Sciences, University of California, Los Angeles, California, and Jet Propulsion Laboratory, California Institute of Technology, Pasadena, California; DAVIES—Jet Propulsion Laboratory, California Institute of Technology, Pasadena, California; AVERILL—Raytheon Corporation, Information Technology and Scientific Services, and Jet Propulsion Laboratory, California Institute of Technology, Pasadena, California; WESTPHAL—Department of Geological and Planetary Sciences, California Institute of Technology, Pasadena, California
CORRESPONDING AUTHOR: Michael J. Garay, Department of Atmospheric and Oceanic Sciences, University of California, Los Angeles, 405 Hilgard Avenue, Box 951565, 7127 Math Sciences Building, Los Angeles, CA 90095-1565
E-mail: garay@atmos.ucla.edu
DOI:10.1175/BAMS-85-10-1585

In final form 11 April 2004

vective systems are also of interest because they reveal complex and poorly understood processes that affect cloud appearance and behavior in regions that play a significant role in the global climate system, particularly the tropical oceans (e.g., Blaskovic et al. 1991; Klein and Hartmann 1993).

This paper describes *actinoform* clouds, a class of shallow convective cloud systems that show an incredible degree of self-organization, which are often left out of cloud typologies. It is not generally known that these systems have been observed in satellite images as far back as the 1960s and were described in the pages of both the *Monthly Weather Review* (e.g., Picture of the Month, 1963, Vol. 93, p. 212) and *Bulletin of the American Meteorological Society* (Agee 1984). In fact, this particular class of clouds is not mentioned in the second edition of the *Glossary of Meteorology* (Glickman 2000). We will show that actinoform clouds are surprisingly common in certain regions of the world and that some of the early theories regarding these clouds are probably incorrect.

BACKGROUND. Soon after the launch of the first *Television Infrared Observation Satellite* (*TIROS I*), shallow hexagonal cloud cells with diameters of 50–100 km were reported by Krueger and Fritz (1961). As satellite observations accumulated, it became apparent that shallow convective systems were often organized into *cells* of cloudiness. This phenomenon came to be known as "mesoscale cellular convection" (MCC; Hubert 1966).[1]

MCC is divided into two basic types, open and closed, based on whether or not the center of the cell is clear or cloudy. It is important to realize that, when discussing MCC, a cloud "cell" does not refer to an individual cloud, but rather to a system of associated clouds. Figure 1 shows examples of the two types. From their first description by Kreuger and Fritz (1961), it was noted that the organization of these shallow convective cells bore a striking resemblance to Rayleigh–Bénard convection, which is easily produced in the laboratory by heating a shallow layer of fluid from below and cooling it from above. A great deal of work has been done both observationally and theoretically to understand the relationships between MCC and Rayleigh–Bénard convection. The extensive literature on MCC has been reviewed by Agee (1984) and Atkinson and Zhang (1996).

A third class of MCC, which does not fit into either of the other two categories, was first observed in images from *TIROS V*, launched in 1962. One of these images (Fig. 2b) was striking enough to become the very first feature of the *Monthly Weather Review*'s Picture of the Month series, which began in January 1963 (Vol. 93, p. 32). The text accompanying that first Picture of the Month identified these cloud systems as actinoform clouds, where, as with other types of MCC, the term refers to the collection of clouds and not to any individual cloud. The radial arms of convective cloudiness in these systems are known as *actiniae* (Agee 1984). Following the precedent established by Howard, actinoform clouds derive their name from their appearance. The base "actino-"

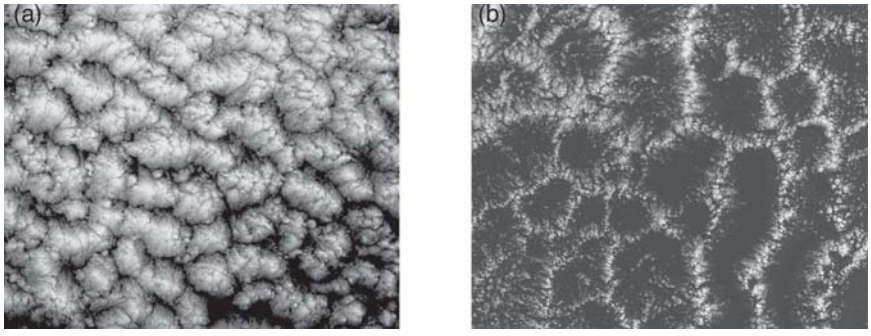

FIG. 1. (a) An example of closed MCC obtained from the MISR instrument (Diner et al. 1998) on the *Terra* satellite on 15 Aug 2002 at a latitude of 15°S and a longitude of 98°W. The *Terra* satellite has an equatorial crossing time of approximately 10:30 A.M. local time (or LT). The nominal resolution of the MISR instrument is 275 m in four color bands for the nadir-looking (An) camera (Diner et al. 1998). The dimensions of the image are approximately 200 km in both directions (north is toward the top of the image). Closed cells form when moist air rises in the center of the cell-forming clouds. Air at the edges of the cells descends, causing clearing. (b) An example of open MCC from MISR obtained on 1 Aug 2002: latitude 30°S, longitude 0°E. The width of the image is approximately 280 km. Large, somewhat irregular, hexagonal cells are clearly visible. Air rises at the cell boundaries in open cells, forming clouds, and descends in the clear center.

[1] The designations mesoscale cellular convection and MCC have a historical tradition within the meteorological satellite community dating back at least to Hubert (1966). Care must be taken to avoid confusion with the much more recent and common usage within the literature of MCC to refer to "mesoscale convective complex," as introduced by Maddox (1980).

comes from the Greek[2] word for "ray" (which also serves as the base for the name of the radioactive element actinium).

Reports of actinoform clouds were relatively infrequent, as indicated by Fig. 2, which shows nearly every image of actinoform clouds acquired over a period of almost 30 yr, with a single, notable exception (it has come to our attention that a 1997 study of an actinoform cloud feature can be found online at http://cimss.ssec.wisc.edu/wxwise/swirl/actinae2.htm). A rather poor-quality image of an actinoform cloud obtained by the Advanced Vidicon Camera System (AVCS) on the *Nimbus-1* satellite made its first appearance in Hubert (1966). This same image was reproduced by Agee (1984) in his review of MCC and last appeared in a textbook on cloud dynamics by Houze (1993, p. 171). In spite of (or perhaps because of) the lack of observations, the explanation was advanced that actinoform clouds represent a transitional form between closed and open cells. As a result, most MCC research, as described by Agee (1984) and Atkinson and Zhang (1996), has focused on understanding open and closed MCC systems. In fact, the review by Atkinson and Zhang (1996) does not mention the existence of actinoform clouds and, as stated earlier, the term has become so obscure that it is not included in the up-

[2] It is amusing to note that in this case a Greek base was used, while Howard had been a strong advocate for the exclusive use of Latin bases for cloud names (Hamblyn 2001).

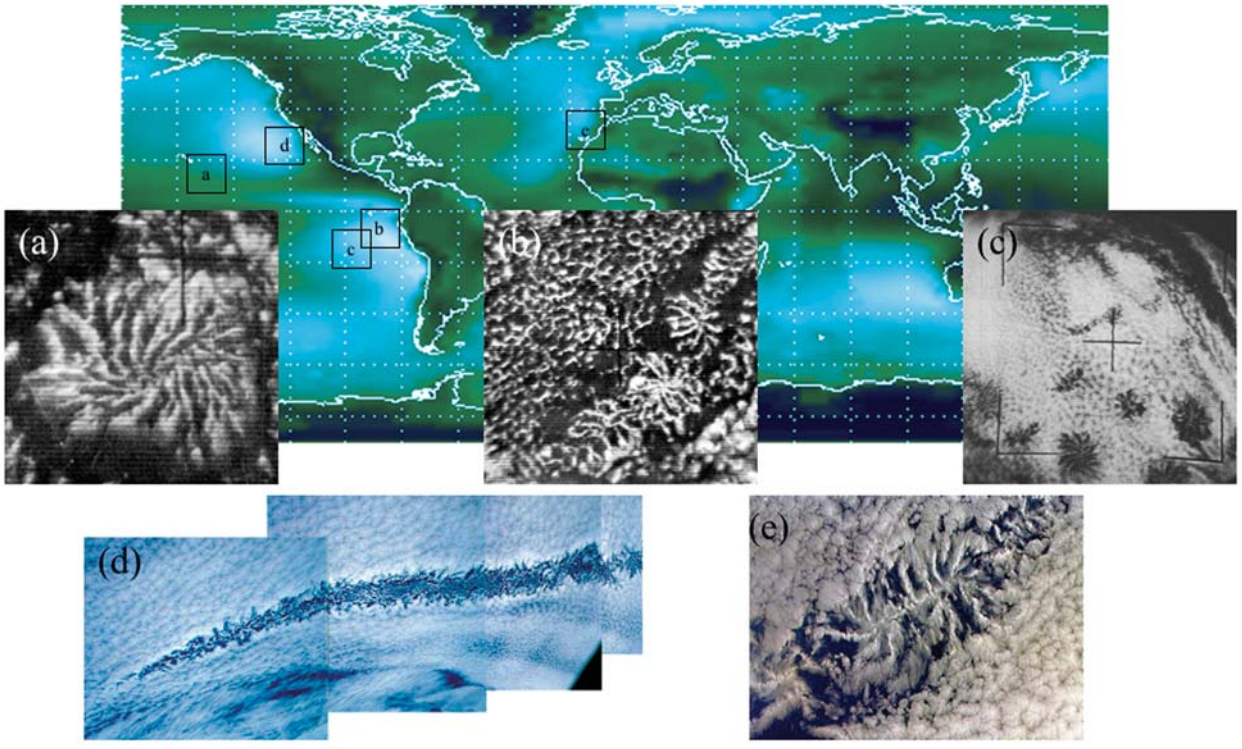

Fig. 2. (Map) International Satellite Cloud Climatology Project (ISCCP) D2 1983–2001 mean annual low-cloud amount (cloud-top pressure greater than 68 kPa). Bright regions indicate higher percentages (up to 60%) of low-cloud occurrence (see Rossow et al. 1996). (a) First satellite image of an actinoform cloud from *TIROS V* (2322 UTC 16 Aug 1963, 17.5°N, 155°W). Cloud is over 300 km in diameter (Picture of the Month in *Mon. Wea. Rev.* 1965, Vol. 93, p. 212; available online at www.photolib.noaa.gov/space/spac0162.htm). (b) First Picture of the Month image (*Mon. Wea. Rev.* 1963, Vol. 91, p. 2, available online at www.photolib.noaa.gov/space/spac0160.htm). Series of actinoform clouds observed by *TIROS V* (1500 UTC 7 Oct 1962, 7°S, 87°–97°W). (c) Picture of the Month April 1965 (*Mon. Wea. Rev.*, Vol. 93, p. 212). Actinoform clouds from *TIROS VIII* (1713 UTC 18 Jul 1964, 15°S, 100°W, available online at www.photolib.noaa.gov/space/spac0161.htm). (d) Composite of four photographs by astronaut from space (STS51G-31-10 to -13). Cloud feature extends hundreds of kilometers (1600 UTC 17 Jun 1985, 27°N, 122°–118°W). (e) Detail of astronaut photograph STS043-96-54 showing actinoform cloud northeast of Canary Islands (0800 UTC 7 Aug 1991, 26°N, 16.5°W). Astronaut images courtesy of the Earth Sciences and Image Analysis Laboratory, NASA Johnson Space Center (online at http://eol.jsc.nasa.gov).

dated second edition of the *Glossary of Meteorology* (Glickman 2000).

This was the situation in 2001 when MISR (Diner et al. 1998) was launched on the National Aeronautics and Space Administration (NASA)'s polar-orbiting *Terra* satellite and it happened to pass nearly directly over a particularly distinctive actinoform cloud (Fig. 3a). By coincidence, the cloud filled nearly the entire width of MISR's 380-km image swath. Subsequent searches through a very small fraction of the MISR data obtained since 2000 have revealed in excess of 50 easily identifiable cases of actinoform clouds in various regions of the world. Other examples have been collected in GOES imagery. Figure 3 shows a sampling of actinoform clouds from the MISR dataset. Far from being rare, actinoform clouds have been identified in nearly every region of the world where marine stratus or stratocumulus are common.

CASE STUDY. In order to illustrate some of the important characteristics of actinoform clouds as revealed by the newest generation of satellite instruments, we focus on the first actinoform cloud found in the MISR data at 1700 UTC 16 November 2001 (Fig. 3a). The location of the cloud is indicated by the box marked with the letter "a" on the map in Fig. 3. This part of the eastern Pacific is under the influence of the cold Peruvian Current, which flows from Antarctica northward along the western coast of South America. In addition, the region is located in the descending branch of the equatorial Hadley cell, an extensive region of high pressure resulting in a shallow boundary layer capped by a strong and dry temperature inversion. Visual inspection of 50 MISR orbital passes, which occur once every 16 days, over this rather narrow region (MISR path 21) from 9 June 2001 to 2 August 2002 revealed the presence of actinoform clouds (or related complex cloud features)

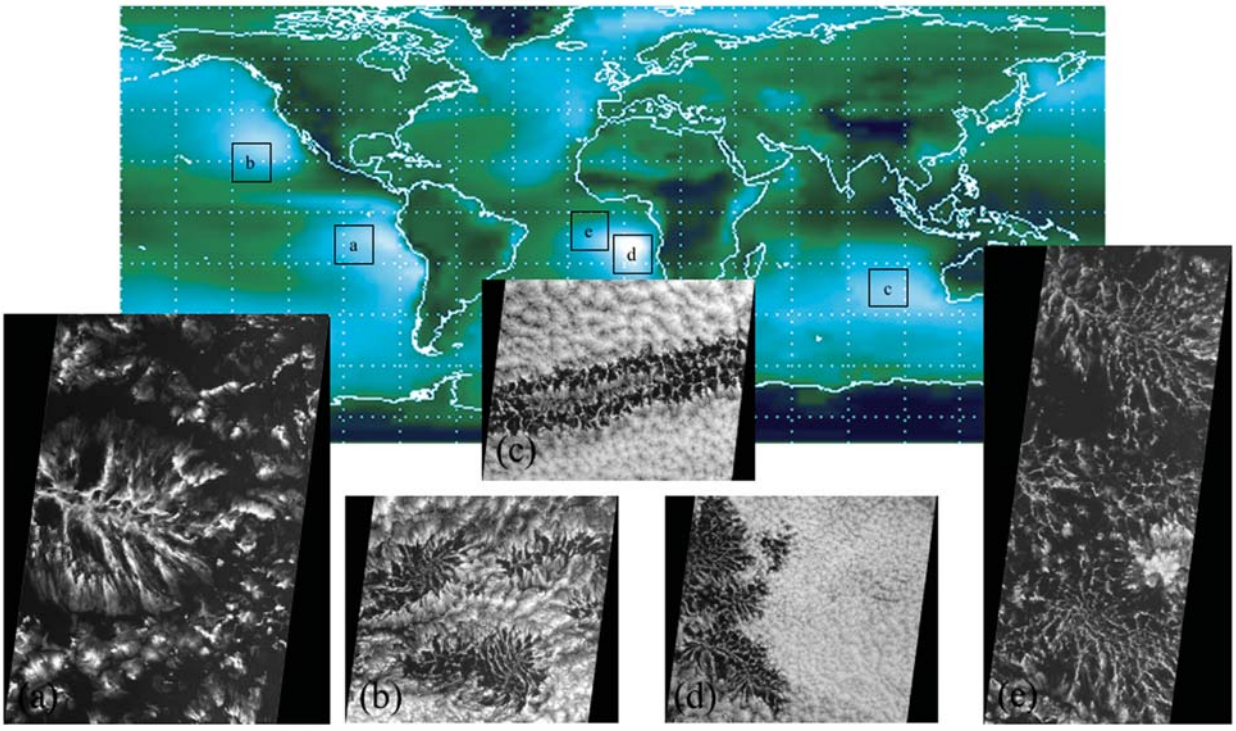

Fig. 3. (Map) ISCCP D2 1983–2001 mean annual low-cloud amount (see Fig. 2). (a) MISR image of an actinoform cloud (1700 UTC 16 Nov 2001, 13°S, 98°W). Width of the MISR swath is 380 km. This cloud, which looks very much like a leaf, was seen in a brief survey of the MISR low-resolution browse images. Its identification prompted a search for more examples of this type of cloud in the MISR data. (b) MISR image of "negative" leaves (1947 UTC 23 Jun 2002, 18°N, 136°W). This image closely resembles Fig. 2a, the first actinoform cloud observed from space. (c) MISR image of a "double millipede" hinting at the complexity that can arise in the marine boundary layer (0415 UTC 26 July 2002, 30°S, 89°E). (d) MISR image of "spiders" (1009 UTC 1 Aug 2002, 13°S, 4°E). Comparison of this image with the others shows that the relative position of actinoform features can take any number of configurations. (e) A second MISR image of "spiders" (1121 UTC 27 Aug 2001, 9°S, 12°W). Center to center, these two similar cloud features are nearly 700 km apart.

in 12 cases (24%), which implies that actinoform clouds are quite common here.

Data. Because observational data are scarce in this part of the Pacific, our investigation relies primarily on satellite images obtained during the 1700 UTC overpass of the MISR instrument on the polar-orbiting *Terra* satellite. The MISR data were obtained from the NASA Langley Research Center Atmospheric Sciences Data Center. MISR provides spatial resolution of up to 275 m in nine cameras with viewing angles relative to satellite nadir of 0°, ±26.1°, ±45.6°, ±60.0°, and ±70.5° (Diner et al. 1998). To provide temporal coverage, GOES-West (Menzel and Purdom 1994) 3-hourly full-disk 1-km visible (0.65 μm) and 4-km infrared (10.7 μm) images were obtained directly from the satellite by a ground station located at the University of Arizona in Tucson. In addition, National Centers for Environmental Prediction (NCEP)–National Center for Atmospheric Research (NCAR) global reanalysis data (Kalnay et al. 1996) were obtained from the National Oceanic and Atmospheric Administration (NOAA)–Cooperative Institute for Research in Environmental Sciences (CIRES) Climate Diagnostics Center in Boulder, Colorado (from their Web site online at www.cdc.noaa.gov).

Results. Figure 4a shows the 1700 UTC MISR image of the actinoform cloud and Fig. 4b shows the GOES-West image obtained 1 h later at 1800 UTC. The much higher resolution MISR image reveals the complex self-organization that constitutes the actinoform cloud. A number of radial arms, or actiniae, are readily identified in the image. The actinoform cloud is separated from a surrounding group of closed MCC cells by a region of clear air. The lower-resolution GOES image has a slightly different viewing geometry compared to the MISR image, which accounts for some of the differences between the two. In addition, some evolution of the actinoform cloud in the intervening hour is apparent, particularly in the northeast part of the system where some cloud development has taken place. The ring of clear air also appears to have grown larger, but the overall organization of the system is still very much the same.

Linear dimensions for the actinoform cloud are included in Fig. 4b. These measurements compare favorably with a diameter of 323 km for the actinoform cloud shown in Fig. 2a and diameters of approximately 200 km for the actinoform clouds shown in Fig. 2b. Observing cloud features with diameters of 300 km from space may not seem particularly surprising. However, calculation of the areal

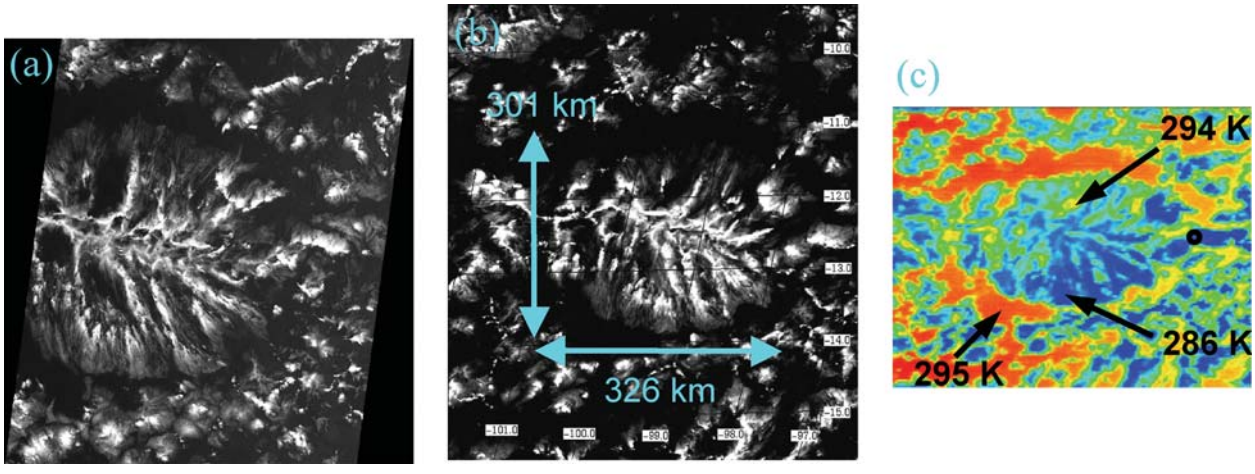

Fig. 4. (a) Detail of Fig. 3a. Image of actinoform cloud obtained by MISR at 1700 UTC 16 Nov 2001. MISR's An camera has a pixel resolution of 275 m and the width of the image swath is 380 km. (b) GOES-West grayscale visible channel (0.65 μm) image of the cloud shown in (a) at 1800 UTC. The pixel resolution of GOES is approximately 1 km (Menzel and Purdom 1994). Latitude and longitude lines have been superimposed. Linear dimensions are indicated on the figure. Assuming the cloud feature is elliptical, the area of the cloud is 77,000 km^2, nearly the size of the state of South Carolina. (c) GOES-West 10.7-μm IR false color image of the cloud in (a) and (b). The resolution of the GOES 10.7-μm channel is 4 km. Effective temperatures derived from the 10.7-μm brightness temperatures by matching the values to the NCEP–NCAR reanalysis sea surface temperature are indicated on the image. The coldest observed cloud tops are 9 K colder than the sea surface. The location of the nearest NCEP–NCAR reanalysis grid point is indicated by the black circle to the east of the actinoform cloud.

coverage of these clouds is another matter. If we assume the cloud shown in Fig. 4 is elliptical, this yields an area of 77,000 km^2, which is nearly the size of the state of South Carolina! By comparison, the cloud in Fig. 2a has a circular area of 81,700 km^2 and the cloud features shown in Fig. 2b have areas of approximately 32,000 km^2. This suggests that the cloud observed on 16 November 2001 is not unusually large because it falls within the parameters of previously observed actinoform clouds.

In addition to knowing the size of the cloud, it is useful to know its height as well. Because it views a scene from multiple angles, MISR is able to use a stereophotogrammetric technique to retrieve cloud-top heights (Moroney et al. 2002). In this case, the MISR retrievals indicate that the cloud top is approximately 1.5 km above the surface.

GOES-West 10.7-μm channel imagery shown in Fig. 4c provides brightness temperatures from which the height of the cloud top can also be estimated. It should be noted that even at the reduced resolution of the 10.7-μm data (which has pixels 16 times larger than the GOES visible channel pixels and over 200 times larger than the MISR nadir camera pixels), the structure of the actinoform cloud is still apparent and there are regions within the cloud where the brightness temperatures indicate that the sea surface can be seen between individual cloud elements. The 10.7-μm brightness temperatures were calculated from the GOES radiances and were then adjusted to match the sea surface temperatures from the 1800 UTC NCEP–NCAR global reanalysis (Kalnay et al. 1996) at the grid point shown by the black circle to the right of the cloud in Fig. 4c. The maximum brightness temperature difference in the scene is 9 K. Comparing the adjusted brightness temperatures with the temperature profile derived from the reanalysis data indicates that the cloud has a maximum height of approximately 1.4 km above the surface. This result agrees well with the MISR stereo retrieval and shows that the individual convective clouds that collectively make up the actinoform cloud are indeed quite shallow, as would be expected for MCC.

To track the temporal evolution of the cloud system, we obtained GOES-West visible images for 1800 UTC from 12 to 17 November 2001. This sequence is shown in Fig. 5. The western coast of South America, including Chile and Peru, can be seen along the extreme right edge of each of the images. By way of reference, the actinoform cloud observed by MISR on 16 November is indicated by the arrow in Fig. 5e. It appears that some sort of "disturbance" occurred in the marine boundary layer 4 days earlier on 12 November, as shown in Fig. 5a. On this day, the region was dominated by closed MCC, except for a small region just off the coast of Chile in the lower right-hand corner of the image. Figure 5b shows that on 13 November (24 h later) the disturbance had propagated to the northwest, and self-organized features began to appear as the nature of the MCC in the region was altered. By 14 November (Fig. 5c), the region from which the MISR actinoform cloud originated is easily identified. The boundary layer disturbance continued to propagate to the northwest, and longer, more linear features are evident. By the next day, a series of actinoform cloud lines formed (Fig. 5d). The complex that developed into the actinoform cloud observed by MISR is very clear, but became better organized the following day, as shown in Fig. 5e. This view shows that the actinoform cloud is part of an even larger organization, which is very similar to the cloud system shown in Fig. 2b, observed in nearly the same region of the globe over 40 yr earlier. Other actinoform clouds, though less well defined, can be seen to the west and east of the one imaged by MISR. The total length of this "train" of actinoform clouds is on the order of 2,000 km, or greater than 6 times the linear dimension of the original cloud. However, by 17 November (Fig. 5f) the actinoform organization disappeared entirely from the region, although some hint of large-scale linear organization remains. It is even difficult to pinpoint precisely the location of the cloud elements that had made up the well-organized actinoform cloud feature on the previous day.

Finally, an average motion of 10 m s^{-1} for the clouds was determined via manual tracking of the cloud features using the 3-hourly GOES-West visible data. This value is consistent with the monthly climatology of the winds in the region according to the NCEP–NCAR reanalysis data for November 2001. The cloud motion speed is also consistent with the reanalysis data from 16 November 2001 for the model grid point indicated by the circle in Fig. 4c. The total wind speed derived from these data is between 10.0 and 11.4 m s^{-1} from 101.1 to 85 kPa (the surface to an altitude of 1500 m).

DISCUSSION. The linear nature of the cloud features shown in Fig. 5 indicates that whatever the mechanism that results in actinoform cloud organization, it operates on a variety of spatial scales. Individual convective clouds organize themselves into radial structures at intermediate scales, and lines of these radial structures are organized at even larger scales. Interestingly, linear features associated with

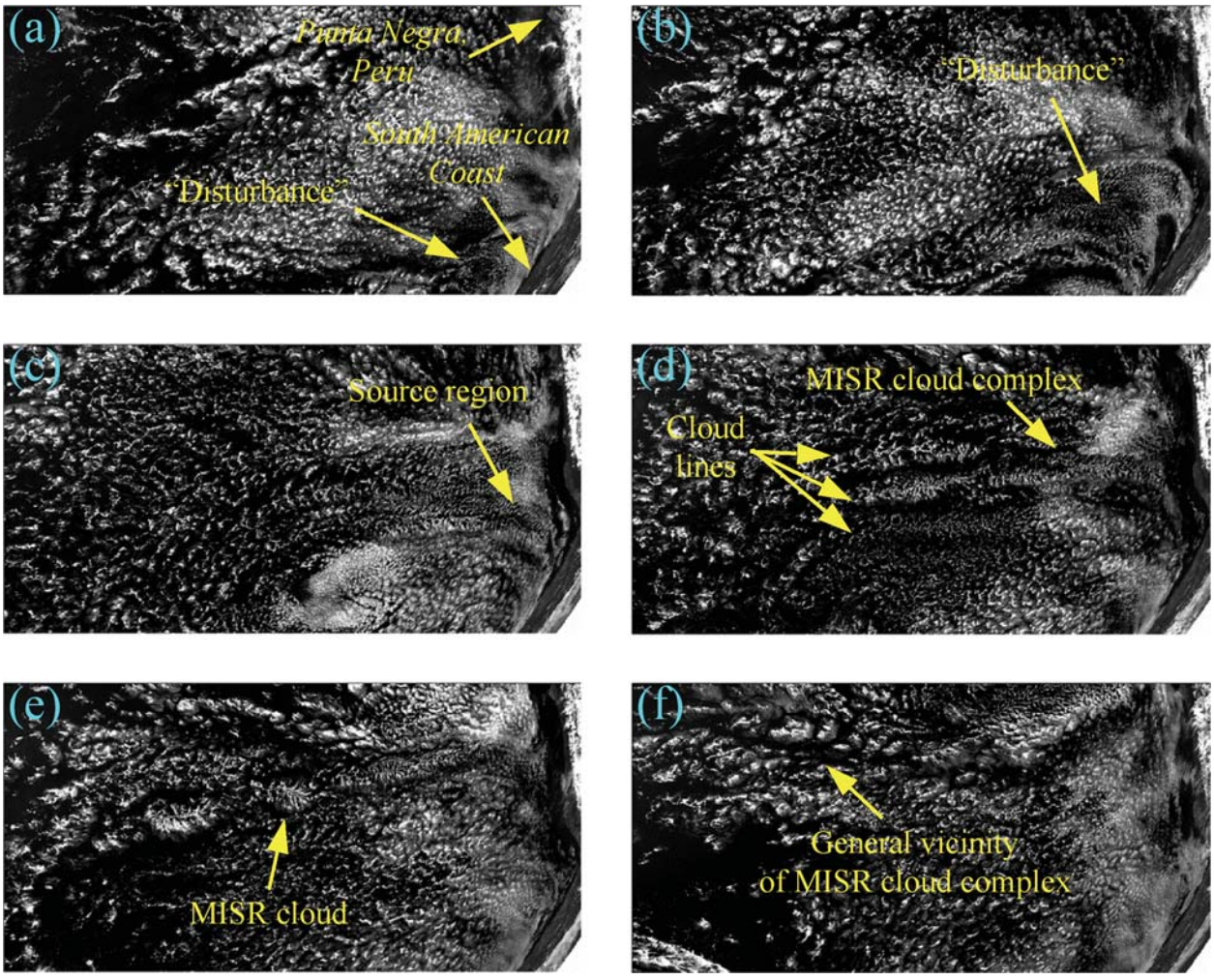

FIG. 5. Sequence of visible images (0.65 μm) at 1-km resolution from GOES-West obtained at 1800 UTC on consecutive days from 12 to 17 Nov 2001. (a) 1800 UTC 12 Nov image. The origin of the complex that led to the formation of the actinoform cloud observed by MISR is in the lower right corner of the image. (b) 1800 UTC 13 Nov image. The boundary layer disturbance has propagated to the northwest. Associated actinoform cloud features begin to appear. (c) 1800 UTC 14 Nov image. Linear bands of actinoform clouds begin to appear. The MISR cloud complex itself can be identified in this image. (d) 1800 UTC 15 Nov image. The MISR cloud complex has propagated further to the northwest, away from the coast of Peru. Clear lines of actinoform cloudiness are apparent. (e) 1800 UTC 16 Nov image. The actinoform cloud that was observed by MISR is indicated by the arrow. (f) 1800 UTC 17 Nov image. In 24 h the organization that had persisted for at least 3 days has dissipated. The general vicinity of the actinoform cloud complex obtained by extrapolating its motion forward from the previous image is indicated by the arrow.

tropical convection were previously noted in historical satellite data. A comparison of two images (Figs. 6a and 6b) from *TIROS III,* which appeared as the Picture of the Month in the May 1963 issue of *Monthly Weather Review* (Vol. 93, p. 306; with the relevant image from the sequence in Fig. 5 as Fig. 6c), is shown in Fig. 6. The similarity of the three images suggests that such organized, linear features are common in the tropical oceans throughout the world.

One obvious conclusion that may be drawn is that large-scale linear collections of actinoform clouds are linked in some way to ocean currents. This relationship would be consistent with the climatology of open and closed MCC produced by Agee (1984), which shows that closed cells tend to be associated with cool ocean currents to the west of continents and open cells tend to be associated with warmer waters. The Peruvian Current, which is a cool, low-salinity current influenced by offshore winds flowing north along the coast of Chile and Peru, is the dominant current in the region where we have found actinoform clouds to be rather common. Yet the fact that the cloud for-

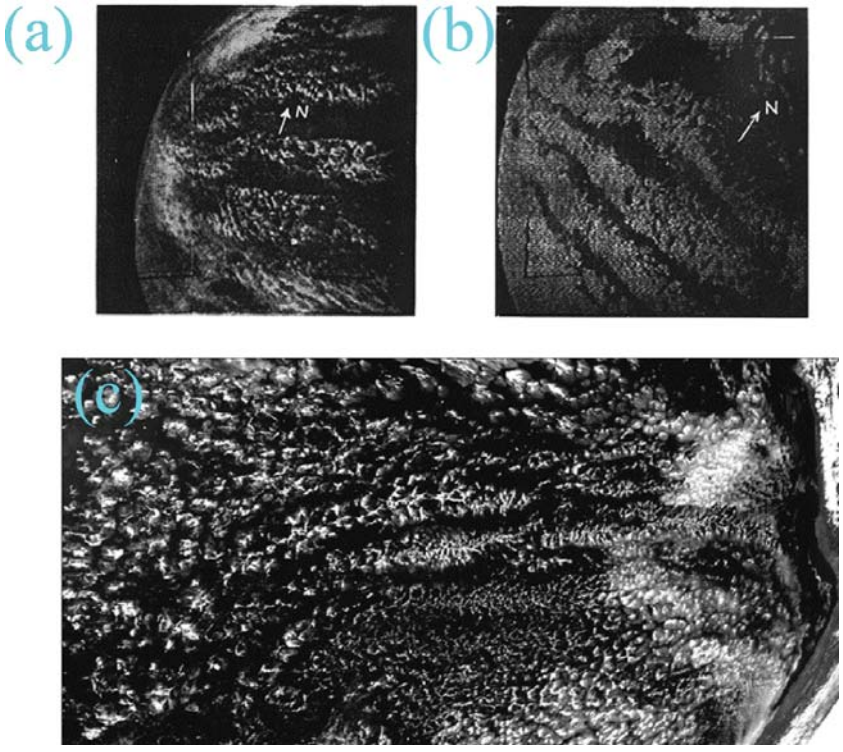

Fig. 6. (a) *TIROS III* image of the southern Indian Ocean, northeast of Madagascar obtained at 0620 UTC 26 Jul 1961 (8°–20°S, 50°–70°E). (b) *TIROS III* image midway between Africa and South America obtained at 1203 UTC 28 Sep 1961 (5°–15°S, 5°–30°W). Both (a) and (b) appeared as the Picture of the Month in *Mon. Wea. Rev.* in May 1963 (Vol. 93, p. 306). The author of the feature raised the question, "what is the nature of this remarkable tropical convergence?" (c) GOES-West image from the eastern, central Pacific obtained at 1800 UTC 15 Nov 2001 (10°–25°S, 75°–100°W).

mations do not track the location of the Peruvian Current in the eastern Pacific suggests that no simple relationship exists between actinoform clouds and currents.

However, sea surface temperatures do seem to have some role because they increase quite dramatically from east to west in this region. Similarly, the GOES 10.7-μm brightness temperatures from 16 November give an estimated east–west temperature gradient of +2.4 x 10^{-3} K km^{-1} across the eastern Pacific in the region of the linear cloud features. While the cloud system motion was not constant, the local wind speed of 10 m s^{-1} implies a warming of the associated boundary layer of +2 K day^{-1}. It is clear that the large-scale dynamics involve a complex and poorly understood interplay among the currents, the sea surface temperatures, and the winds.

In turn, the clouds have a complicated effect on the radiation budget of the region. The estimated optical depth obtained from MISR for the entire actinoform cloud system is approximately 4. However, the optical depths of individual cloud elements have been found to range from 1 to 70. Effective albedos estimated from GOES yield a mean of 13% with a range from 2% for the darkest clear ocean surface, to 58% for the thickest clouds in this region. Overall, the albedos have quite a large variance, which has significant consequences for calculations of the local radiation budget. The average monthly mean clear-sky downward solar flux from the NCEP–NCAR reanalysis for November 2001 in the region is 379 W m^{-2}. The estimated albedos imply that surface absorption of downwelling solar radiation can differ by over 200 W m^{-2} in this area, due to the broken nature of the actinoform cloud field. This broken nature also makes the operational retrievals of cloud parameters using the Moderate Resolution Imaging Spectroradiometer (MODIS; Platnick et al. 2003) problematic.

Our findings further suggest that the long lifetime of the actinoform cloud features—up to 72 h in some cases—allows for plenty of time for processes, such as drizzle (Stevens et al. 2004; van Zanten et al. 2004) and longwave cooling (Guan et al. 1997), to influence the dynamics within the actinoform cloud system. At the same time, large-scale dynamics must also be important because the overall organization can be maintained for a number of days.

Previous theories. Hubert (1966) originally suggested that actinoform clouds are a transitional form between open and closed MCC. This idea was repeated by Agee (1984) and Houze (1993).[3] However, as we have seen in the case of 16 November 2001, the actinoform clouds observed by MISR and GOES are clearly not transitional forms. Moreover, the lack of

[3] It is apparent from the references that this idea seems to have accompanied the *Nimbus-1* AVCS actinoform cloud picture.

open cells in the numerous cases shown in both Figs. 2 and 3 make it difficult to see how actinoform clouds play a transitional role. In fact, with the exception of Fig. 2b, actinoform clouds appear to be more prominently associated with closed MCC than with open cells.

The author of the original Picture of the Month article in *Monthly Weather Review* (Vol. 91, p. 2) summarized the knowledge of actinoform clouds in five points. First, all examples occurred in the Tropics or subtropics. We have also found this to be the case. Second, all examples occurred where there was likely an inversion. This point is borne out by the locations of most of the observed actinoform clouds in the descending branch of the equatorial Hadley circulation and our analysis of the 16 November 2001 case. Third, the size of the patterns ranged from 200 to 320 km in diameter. The cloud observed by MISR falls neatly within this range. Fourth, the cloud type in the region was associated with low-level inversions; this is just another way of saying that actinoform clouds are associated with MCC. Finally, the observation was made that the radial arms—the actiniae—had a tendency to curve clockwise outward in the Northern Hemisphere and counterclockwise outward in the Southern Hemisphere. If this curvature is due to the Coriolis force, then this observation suggests that there is some motion outward from the center of the actinoform cloud itself, although given the scale and depth of the cloud systems in question, it is difficult to imagine how this could occur. In fact, a difference in the direction of curvature is contradicted by Fig. 7. Figure 7a shows an example of an actinoform cloud from the Northern Hemisphere (18°N) and Fig. 7b shows another example of an actinoform cloud from the Southern Hemisphere (13°S). Even with the superior resolution of MISR relative to older satellite instruments, it is difficult to assess the presence of any "curvature." The two images in Fig. 7 are essentially indistinguishable. Large-scale rotation of a few actinoform cloud systems is apparent based on inspection of both GOES image sequences and MISR camera animations (representing the evolution of the cloud system on time scales on the order of minutes), but, somewhat surprisingly, most of these systems, in fact, do not appear to be rotating.

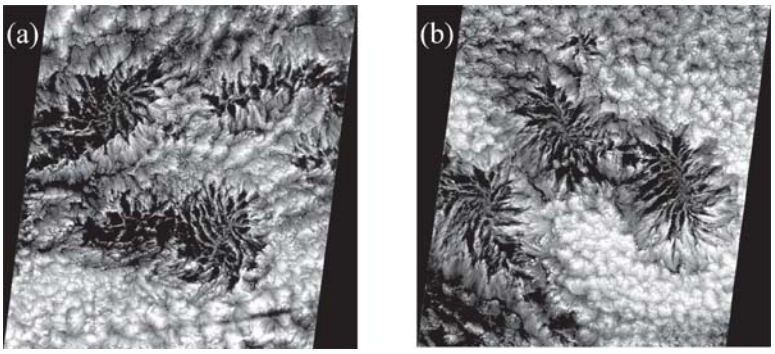

Fig. 7. Two examples of actinoform clouds from MISR data. (a) A Northern Hemisphere example: 1947 UTC 23 Jun 2002, 18°N, 136°W. (b) A Southern Hemisphere example: 1009 UTC 1 Aug 2001, 13°S, 4°E. The two cases, although from different hemispheres, are essentially identical.

FUTURE WORK. Ongoing and future work involves a broader study of actinoform clouds and related shallow convective cloud features. We are in the process of constructing a more definitive classification and climatology using the available MISR data. Data from recent field campaigns, including the Dynamics and Chemistry of Marine Stratocumulus (DYCOMS)-II (Stevens et al. 2003) and the East Pacific Investigation of Climate Processes in the Coupled Ocean-Atmosphere System (EPIC; Bretherton et al. 2004) should provide useful information on the local conditions that lead to the formation of actinoform cloud patterns.

CONCLUSIONS. In developing his cloud classification, Howard discovered that all clouds followed some underlying organizational principle. The shapes clouds took were not completely random. This allowed him to characterize the clouds by the forms they typically assume. Recent satellite observations have rediscovered unexpectedly complex cases of cloud self-organization on a much larger scale than Howard had imagined. The exploration of this organization and attempts to understand its underlying cause may lead us to important new insights about our atmosphere.

ACKNOWLEDGMENTS. The research described in this paper was performed at the Jet Propulsion Laboratory, California Institute of Technology, under a contract with the National Aeronautics and Space Administration.

We would like to thank Shawn Ewald for his assistance in compiling a GOES database of actinoform clouds. Special thanks to David J. Diner for his continual support of this effort. Additional thanks is due to James F. W. Purdom for his insightful comments and for his GOES animations of an actinoform cloud case. Finally, a number of reviewers helped improve the clarity of the manu-

script and, in particular, pointed out the online study of a 1997 actinoform cloud case referenced in the paper.

REFERENCES

Agee, E. M., 1984: Observations from space and thermal convection: A historical perspective. *Bull. Amer. Meteor. Soc.,* **65,** 938–949.

Atkinson, B. W., and J. W. Zhang, 1996: Mesoscale shallow convection in the atmosphere. *Rev. Geophys.,* **34,** 403–431.

Blaskovic, M., R. Davies, and J. B. Snider, 1991: Diurnal variation of marine stratocumulus over San Nicolas Island. *Mon. Wea. Rev.,* **119,** 1469–1478.

Bretherton, C. S., and Coauthors, 2004: The EPIC 2001 stratocumulus study. *Bull. Amer. Meteor. Soc.,* **85,** 967–977.

Diner, D. J., and Coauthors, 1998: Multiangle Imaging Spectroradiometer (MISR) instrument description and experiment overview. *IEEE Trans. Geosci. Remote Sens.,* **36,** 1072–1087.

Glickman, T. S., Ed., 2000: *Glossary of Meteorology.* 2d ed. Amer. Meteor. Soc., 855 pp.

Guan, H., M. K. Yau, and R. Davies, 1997: The effects of longwave radiation in a small cumulus cloud. *J. Atmos. Sci.,* **54,** 2201–2214.

Hamblyn, R., 2001: *The Invention of Clouds.* Farrar, Straus, Giroux, 403 pp.

Houze, R. A., Jr., 1993: *Cloud Dynamics.* Academic Press, 573 pp.

Hubert, L. F., 1966: Mesoscale cellular convection. U.S. Department of Commerce, Environmental Science Services Administration, Meteorological Satellite Laboratory Tech. Rep. 37, 68 pp.

Kalnay, E., and Coauthors, 1996: The NCEP/NCAR 40-Year Reanalysis Project. *Bull. Amer. Meteor. Soc.,* **77,** 437–471.

Klein, S. A., and D. L. Hartmann, 1993: The seasonal cycle of low stratiform clouds. *J. Climate,* **6,** 1587–1606.

Krueger, A. F., and S. Fritz, 1961: Cellular cloud patterns revealed by Tiros I. *Tellus,* **13,** 1–7.

Maddox, R. A., 1980: Mesoscale convective complexes. *Bull. Amer. Meteor. Soc.,* **61,** 1374–1387.

Menzel, W. P., and J. F. W. Purdom, 1994: Introducing GOES-I: The first of a new generation of Geostationary Operational Environmental Satellites. *Bull. Amer. Meteor. Soc.,* **75,** 757–781.

Moroney, C., R. Davies, and J.-P. Muller, 2002: Operational retrieval of cloud-top heights using MISR data. *IEEE Trans. Geosci. Remote Sens.,* **40,** 1532–1540.

Orlanski, I., 1975: Rational subdivision of scales for atmospheric processes. *Bull. Amer. Meteor. Soc.,* **56,** 527–530.

Platnick, S., M. D. King, S. A. Ackerman, W. P. Menzel, B. A. Baum, J. C. Riédi, and R. A. Frey, 2003: The MODIS cloud products: Algorithms and examples from Terra. *IEEE Trans. Geosci. Remote Sens.,* **41,** 459–473.

Rossow, W. B., A. W. Walker, D. E. Beuschel, and M. D. Roiter, 1996: International Satellite Cloud Climatology Project (ISCCP) documentation of new cloud datasets. World Climate Research Programme (ICSU and WMO), WMO/TD-737 Geneva, Switzerland, 115 pp. [Available from ISCCP Global Processing Center, NASA GSFC Institute for Space Studies, 2880 Broadway, New York, NY, 10025.]

Stevens, B., and Coauthors, 2003: Dynamics and Chemistry of Marine Stratocumulus—DYCOMS II. *Bull. Amer. Meteor. Soc.,* **84,** 579–593.

——, G. Vali, K. Comstock, R. Wood, M. C. van Zanten, P. H. Austin, C. S. Bretherton, and D. H. Lenschow, 2004: Pockets of open cells (POCs) and drizzle in marine stratocumulus. *Bull. Amer. Meteor. Soc.,* in press.

van Zanten, M. C., B. Stevens, G. Vali, and D. H. Lenschow, 2004: Observations of drizzle in nocturnal marine stratocumulus. *J. Atmos. Sci.,* in press.